JOURNAL OF MATERIALS SCIENCE 26 (1991) 5561–5565

Ceramic composites: TiB_2–TiC–SiC

Part II *Optimization of the composite 20% TiB_2–55% (mol %) TiC–25% SiC*

F. de MESTRAL*, F. THEVENOT
*TURBOMECA, 64511 Bordes, France
Ecole des Mines de Saint-Etienne, 158 Cours Fauriel, 42023 Saint-Etienne Cedex 2, France

The composition 20% TiB_2–55% TiC–25% SiC (mol %) was selected and the hot pressing parameters were optimized using optimal design. The optimized hot-pressed material had a bend strength > 1200 MPa, a thermal shock resistance of 300 °C, and a bend strength at 1200 °C of 456 MPa. The pressureless sintering of the selected composite was optimized, with and without additives. Powders sintered without additives (2200 °C, 2 h) had a low density (92.2%) and strength (480 MPa). Carbon and boron additives led to higher densities (97.5%) but did not improve the strength.

1. Introduction

In Part I [1], mechanical and electrical properties were determined over the complete ternary system TiB_2–TiC–SiC. One particular composition was subsequently selected for a particular application, and its hot-pressing cycle optimized, its high temperature bend strength and thermal shock resistance determined, and its pressureless sintering ability assessed. The results are reported here.

A composition exhibiting high strength and high toughness was selected, and because one potential application could be as heating elements for inert gas furnaces, a third parameter was taken into account: the electrical resistivity. Therefore, the chosen composition had to meet the three following conditions, $\sigma_f > 1000$ MPa, $K_{1c} > 6$ MPa $m^{1/2}$ and $\rho > 50$ μΩ cm (Fig. 1): 20 mol % TiB_2–55 mol % TiC–25 mol % SiC.

2. Hot-pressed material

2.1. Hot-pressing cycle optimization

Our aim was to determine the hot pressing cycle which would achieve full densification at the lowest temperature, pressure and soaking stage. The cycle was composed of two temperature stages, T, with different lengths, t. In addition to these five parameters (T_1, t_1, T_2, t_2, P), six others were taken into account (Table I). The classical ways of studying the effects of eleven parameters require too many experiments: to keep to this we would have to omit the study of some factors, by assuming their influence is negligible. Therefore, we decided to use multifactorial experiment plans (Plackett and Burman matrix [2]) to minimize the number of experiments without neglecting to any parameter. This matrix is given in Table II with the density, open and closed porosity, and bend strength of the resulting materials. The influence of a particular factor (e.g. of the temperature of the first stage) on a response (e.g. on the density) is computed by taking the average of the summation of the studied response rounded-up by the mark given in the factor's column [3]. The constant (mean effect) is the average summation of the studied response and represents the theoretical value of this response, every parameter being set to its middle value (average between low (−) and high (+)). Table III shows that the major parameters are the first stage temperature and the pressure, i.e. the mean density is increased by 2.1% when either the first stage temperature increases from 1750–1800 °C or the pressure rises from 30–40 MPa. On the other hand, the mean density decreases by 0.9% when the increasing pressure rate rises from 0.55–1 MPa s^{-1}. The same trends are maintained for the other responses. Therefore, we conclude that to obtain the best properties, every factor should be set to its high level, except for the moment of applying pressure and the increasing pressure rate, which are set at their low level.

The small influence of second stage temperature is unexpected. A fractional factorial matrix [3] (Table IV) with the four stage parameters is, therefore, carried out with the double objective of studying in more detail the influence of these parameters and to determine if the temperature of maximum densification rate, T_m, is an appropriate densification temperature. For the selected composite, T_m was equal to 1580 °C; this was thus the lowest temperature used in the planned experiments. The influence of the parameters and their interactions (Table V) were computed as for the Plackett matrix. Once again, the major parameter was the temperature of the first stage, T_1, to be set at its high value (1680 °C) to achieve higher densities. This indicates that T_m, is not a crucial temperature as far as hot pressing is concerned. In fact, this densification rate peak is the conjunction of two opponent effects [4]: the increase in the activation of the sintering processes with temperature is balanced by

0022–2461/91 $03.00 + .12

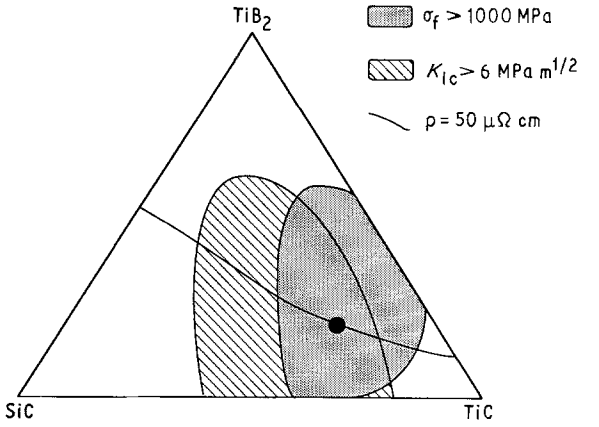

Figure 1 Area in the ternary diagram where the composites meet the three conditions: $\sigma_f > 1000$ MPa, $K_{1c} > 6$ MPa $m^{1/2}$ and $\rho = 50\ \mu\Omega$ cm. (●) The selected composition: 20% TiB_2–55% TiC–25% SiC. (mol %)

the decrease of the densification rate as the porosity tends to close. The influence of the parameters (Table V) and the graphic interpretation of the interactions [5], indicate that each factor should be set to its high value, except for the length of the second stage (the influence of this is nearly negligible so it can be set, indiscriminately, at either its high or low value).

The values chosen for the hot-pressing parameters for the following materials were: first stage temperature, $T_1 = 1750\,^{\circ}C$, duration of first stage, $t_1 = 30$ min, second stage temperature, $T_2 = 1900\,^{\circ}C$, duration of stage length, $t_2 = 15$ min, increasing and decreasing temperature rates $R_{iT} = R_{dT} = 30\,^{\circ}C\ min^{-1}$, pressure, $P = 40$ MPa, the moment of applying pressure, M_p, was the beginning of the hot pressing, the moment of releasing pressure, R_p, was the end of the second stage, increasing pressure rate, $R_{iP} = 0.1$ MPa s^{-1}, decreasing pressure rate, $R_{dP} = 1$ MPa s^{-1}.

2.2. Thermal shock resistance

The thermal shock resistance was determined on samples hot pressed under the latter conditions. The evolution of the bend strength after water quenching as a function of temperature drop, ΔT, is given in Fig. 2. The bend strength of the unquenched sample is higher than that of the non-optimized hot-pressed sample determined in Part I [1] (1230 and 1080 MPa, respectively). This good value is maintained up to a quench of 270 °C. For $\Delta T = 300\,^{\circ}C$, one-third of the samples were damaged thus explaining the very large standard deviation of the measurements. For $\Delta T = 315\,^{\circ}C$, two-thirds of the samples were damaged, and subsequently all the samples deteriorated. Therefore, we conclude that the thermal shock resistance on water quenching the selected composition is 300 °C. This value is in good agreement with that obtained from thermoelastic analysis [6]. Assuming an ideal material where the stresses can be described by Hooke's law, the temperature difference can be estimated by the coefficient R

$$R = \frac{\sigma_R(1 - \nu)}{E\alpha} \quad (1)$$

where σ_R is the strength before thermal shock, i.e. 1200 MPa, ν is Poisson's coefficient, i.e. 0.25, E the

TABLE I Eleven parameters studied for the optimization of the selected composite hot pressing cycle with their high (+) and low (−) values

Parameter			(−)	(+)
T_1	(°C)	first stage temperature	1700	1800
t_1	(min)	first stage duration	15	45
T_2	(°C)	second stage temperature	$T_1 + 50$	$T_1 + 150$
t_2	(min)	second stage duration	5	15
R_{iT}	(°C min^{-1})	increasing temperature rate	10	30
R_{dT}	(°C min^{-1})	decreasing temperature rate	10	30
P	(MPa)	pressure	20	40
M_p	(Mpa)	moment of applying pressure	start	beginning 1st stage
R_p	(Mpa)	moment of releasing pressure	end 2nd stage	at 1000 °C
R_{iP}	(MPa s^{-1})	increasing pressure rate	0.1	1
R_{dP}	(MPa s^{-1})	decreasing pressure rate	0.1	1

TABLE II Plackett matrix for eleven factors and density, D, open, OP, and closed, CP, porosity, and bend strength, σ_f, of the resulting materials

T_1	t_1	T_2	t_2	R_{iT}	R_{dT}	P	M_p	R_p	R_{iP}	R_{dP}	Y	D(%)	OP (%)	CP (%)	σ_f (MPa)
+	+	−	+	+	+	−	−	−	+	−	Y_1	98	0	2	888 ± 54
−	+	+	−	+	+	+	−	−	−	+	Y_2	99.7	0	0.3	1007 ± 92
+	−	+	+	−	+	+	+	−	−	−	Y_3	100	0	0	1017 ± 26
−	+	−	+	+	−	+	+	+	−	−	Y_4	98.5	0	1.5	906 ± 113
−	−	+	−	+	+	−	+	+	+	−	Y_5	92.2	4.8	3	698 ± 14
−	−	−	+	−	+	+	−	+	+	+	Y_6	97.9	0	2.1	904 ± 72
+	−	−	−	+	−	+	+	−	+	+	Y_7	97.3	0	2.7	896 ± 45
+	+	−	−	−	+	−	+	+	−	+	Y_8	98.9	0	1.1	885 ± 68
+	+	+	−	−	−	+	−	+	+	−	Y_9	100	0	0	1003 ± 114
−	+	+	+	−	−	−	+	−	+	+	Y_{10}	90.1	5.7	4.2	758 ± 57
+	−	+	+	+	−	−	−	+	−	+	Y_{11}	99.5	0.3	0.2	1040 ± 26
−	−	−	−	−	−	−	−	−	−	−	Y_{12}	89.4	10.1	0.5	595 ± 30

TABLE III Influence of the different parameters of the hot pressing cycle on the average value (cte) of the density, open and closed porosity, and bend strength

	Density (%)	Open porosity (%)	Closed porosity (%)	Bend strength (%)
cte	*96.8*	*1.75*	*1.5*	*881*
T_1	**2.1**	**− 1.7**	**− 0.5**	**70**
t_1	0.7	− 0.7	0	26
T_2	0.1	0.1	− 0.2	36
t_2	0.5	− 0.8	0.2	34
R_{iT}	0.7	− 0.9	0.2	21
R_{dT}	1	− 1	0	18
P	**2.1**	**− 1.7**	**− 0.4**	**74**
M_p	− 0.6	0	**0.6**	− 21
R_p	0.1	− 0.9	− 0.1	21
R_{iP}	− 0.9	0	**0.9**	− 24
R_{dP}	0.4	− 0.8	0.3	30

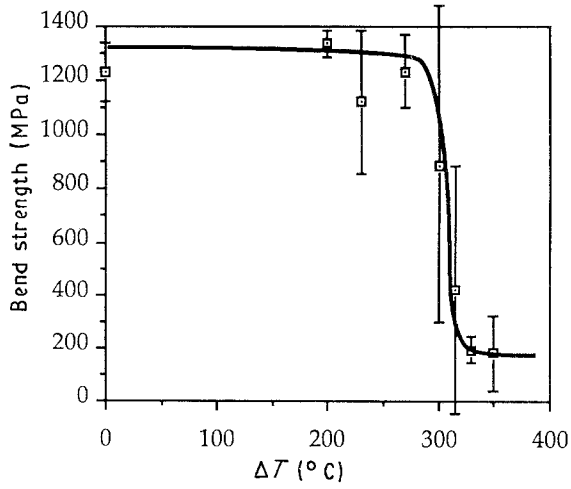

Figure 2 Bend strength of hot-pressed samples after water quenching as a function of the temperature drop.

elastic modulus, i.e. 425 GPa, and α the thermal expansion coefficient, i.e. $7.4 \times 10^{-6}\ K^{-1}$. This leads to $R = 286\ °C$ in our case.

2.3. High-temperature bend strength

The bend strength decreases linearly with increasing temperature (Fig. 3). This is due to the conjunction of two factors. First, the ductile–brittle transition temperature of the main component, TiC, is rather low, i.e. ~ 800 °C [7]. Second, in the tests conducted under nitrogen, there is a surface degradation, e.g. by substitution of carbon by nitrogen in the TiC structure above 800 °C [8]. This degradation, negligible at 800 °C, reaches ~ 10 μm at 1200 °C and ~ 25 μm at 1400 °C.

3. Pressureless sintered material

3.1. Pressureless sintering optimization

The pressureless sinterability of seven grades of the selected composite was studied. The starting powders were mixed either untreated, or after attrition milling, with or without sintering additives (Table VI). To reach a mean particle size of ~ 2 μm, TiB_2 was attrition milled for 8 h and TiC for 4 h. This attrition was followed by a careful wash with hydrochloric acid to remove the iron contamination. Fine SiC was left unmilled. Grade N7, attrition milled, was not washed, so its iron content was as high as 25%. Carbon was added either as black fume, C, or as organic precursor, NL; boron was added as amorphous boron, B, and silicon carbide as organic precursor, polycarbosilane, PC.

In addition to the composition and the sintering additives, pressureless sintering was mainly controlled by the sintering stage temperature and length. A Doelhert matrix [3] was carried out, in order to plot the evolution of the density as a function of these two factors. Table VII lists this matrix and the density of the resulting materials. The first evidence is that grade N7 densifies totally even at the lowest temperature and time. This is due to the liquid-phase formation between Fe and TiC above 1400 °C [8]. The untreated powders (grade N10) only reach the moderate density of 93.3%, but their porosity is nearly totally closed for densities above 90% (open porosity < 0.7%). Polycarbosilane and Novolaque additives are only slightly beneficial in unmilled powders (grade N5). Although native fine and reactive SiC is created, it acts rather as a sintering inhibitor (grade N6), each grain being coated with a thin SiC film, thus disturbing the cohesion between TiC and other components. The best densities are obtained with boron and carbon additives (N3 and N4). However, a sintering temperature of 2100 °C must be reached for boron and carbon to become active. In fact, up to 2100 °C, the milled powders without additives (grade N8) achieve better densification. For the lower temperatures, the milling of powders (grade N4) is beneficial; above 2150 °C, unmilled powders (grade N3) densify in the same way.

TABLE IV Fractional factorial matrix for four factors and density, open porosity, and bend strength, σ_f, of the resulting materials

	T_1 (°C)	t_1 (min)	T_2 (°C)	t_2 (min)		Density (%)	Open porosity (%)	σ_f (MPa)
1	1580 (−)	15 (−)	1580 (−)	5 (−)	Y_1	83.3	16.1	464 ± 26
2	1680 (+)	15 (−)	1680 (−)	15 (+)	Y_2	96.3	0.1	890 ± 68
3	1580 (−)	45 (+)	1580 (−)	15 (+)	Y_3	90.4	8.1	736 ± 26
4	1680 (+)	45 (+)	1680 (−)	5 (−)	Y_4	97.2	0.1	1002 ± 20
5	1580 (−)	15 (−)	1680 (+)	15 (+)	Y_5	93.0	2.9	750 ± 53
6	1680 (+)	15 (−)	1780 (+)	5 (−)	Y_6	97.6	0	1036 ± 44
7	1580 (−)	45 (+)	1680 (+)	5 (−)	Y_7	92.1	4.6	748 ± 65
8	1680 (+)	45 (+)	1780 (+)	15 (+)	Y_8	98.5	0	1037 ± 35

TABLE V Influence of the different parameters T_1, t_1, T_2, t_2, and of their interactions on the average value (cte) of the density, open porosity, and bend strength

	Density (%)	Open porosity (%)	σ_f (MPa)
cte	*93.6*	*3.98*	*834*
T_1	3.85	− 3.92	158
t_1	1	− 0.79	48
T_2	1.75	− 2.09	60
t_2	1	− 1.22	20
$T_1t_1 + T_2t_2$	− 0.55	0.78	− 20
$T_1T_2 + t_1t_2$	− 1.1	2.01	− 15
$T_1t_2 + T_2t_1$	− 1	1.23	− 48

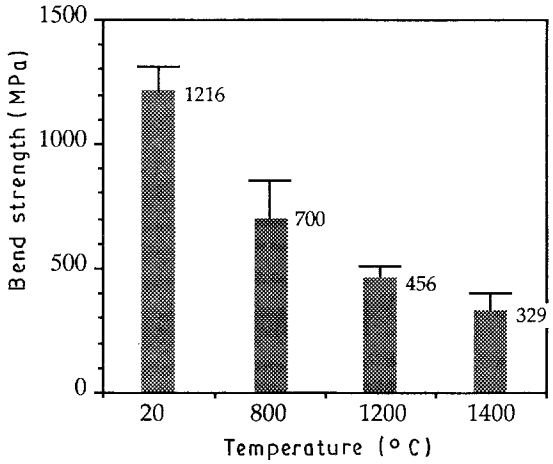

Figure 3 Bend strength evolution of hot-pressed samples at high temperature.

TABLE VI Treatment and sintering additives of the powders

	Powder treatment and sintering additives
N3	Untreated powder + B + C
N4	Attrition milled and cleaned powder + B + C
N5	Untreated powder + PC + NL
N6	Attrition milled and cleaned powder + PC + NL
N7	Attrition milled powder
N8	Attrition milled and cleaned powder
N10	Untreated powder

B: 1% boron; C: 1% carbon; PC: 8% polycarbosilane; NL: 2% novolaque.

A Doelhert matrix allows polynomial models to be developed up to the second order. Although such models are not satisfactory to describe the density evolution of grades N3 and N4, they are satisfactory for grades N5, N6, N8 and N10. However, as the benefit of grades N5, N6 and N8 is very small, only the density evolution of the untreated powders (N10) (Fig. 4) is developed

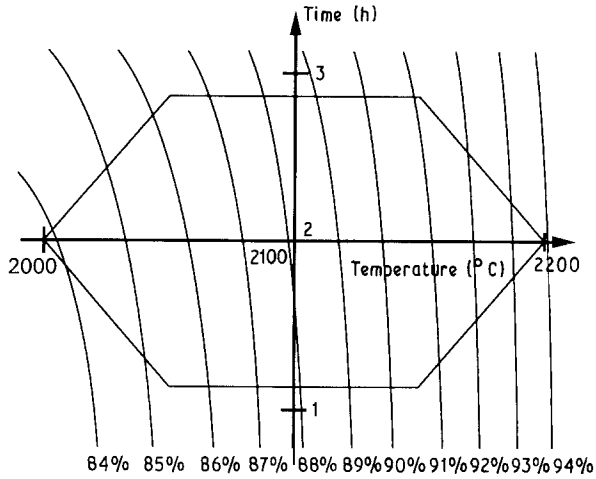

Figure 4 Isodensity curves as a function of the temperature, T, and the duration, t, of the sintering stage, plotted with a second-order polynomial model arising from a Doelhert matrix.

$$Y = 240.9 - 0.199\,T + 4.987\,t + 5.999\,66 \times 10^{-5}\,T^2 + 0.067\,t^2 - 2.309\,39 \times 10^{-3}\,Tt \quad (2)$$

where Y is the density (%), T the temperature (°C) and t the stage duration (h). This model, strictly speaking only valid for $T = 2100 \pm 100$ °C and $t = 2 \pm 1$ h, can be somewhat extrapolated. However, reasonable limits should not be exceeded, e.g. $T = 2100 \pm 200$ °C and $t = 2 \pm 1.5$ h.

3.2. Mechanical characterisations

Mechanical characteristics of grades N10 and N3 were measured. The bend strength of grade N10 (untreated powder) was 484 ± 15 MPa (density 92.2%, open porosity 2.2%, $H_V = 13.9 \pm 2.2$ GPa). Compared with the fully densified hot-pressed material (i.e. 1200 MPa), the strength drop is very large. However, with materials of equal densities, this drop is limited to 210 MPa. This difference is due to grain growth in the pressureless sintered material (Fig. 5). For grade N3, with a density of 97.5% (open porosity 0.1%) and a hardness $H_V = 20.2 \pm 1.8$ GPa, the bend strength was not improved, i.e. 460 ± 46 MPa. This unexpected result is due to the formation of a slight porosity, probably located at the intergranular joints (Fig. 6).

The fracture toughness of these pressureless sintered materials could not be measured. The load necessary

TABLE VII Sintering temperature, T, and time, t, of the Doehlert matrix with the density of the resulting materials

	T (°C)	t (min)	Density (%)						
			N3	N4	N5	N6	N7	N8	N10
1	2100	120	93	**94.5**	92.4	85.4	102	91.8	88.1
2	2000	120	81.1	82.6	81.9	79	102.9	**84.4**	83.7
3	2050	172	86.5	87.9	87.9	83	102.6	**90.7**	86.5
4	2150	172	**97.5**	**97.5**	95.6	87.8	–	94.2	90.8
5	2200	120	**98.2**	**98.2**	96.7	89.8	–	96	93.3
6	2150	67	96.8	**97.1**	94.8	86.9	–	93.5	90.3
7	2050	67	84.2	85.8	85.7	81.4	102.9	**89**	85.6

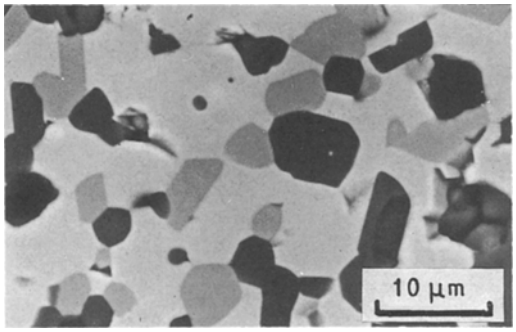

Figure 5 Backscattered electron micrograph of the pressureless sintered material without additives, density 92.2% (grade N10).

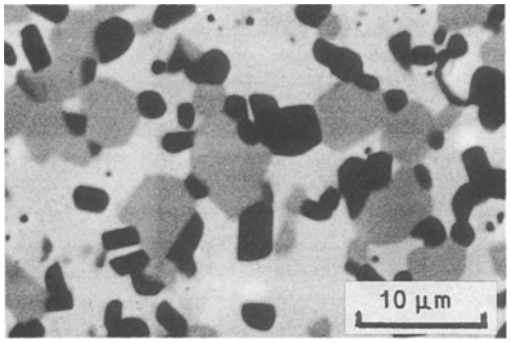

Figure 6 Backscattered electron micrograph of the pressureless sintered material with boron and carbon additives, density 97.5% (grade N3).

to generate cracks was high enough to degrade the indentation itself. The energy applied was not totally used to develop cracks, which were, hence, shortened. The toughness measured under these conditions reach 30 MPa $m^{1/2}$; this is obviously wrong.

4. Conclusion

Research methods using optimal design allowed optimization of eleven parameters of the hot-pressing cycle of a selected composition. The materials produced with this optimized cycle exhibited enhanced bend strength, i.e. $\sigma_f > 1200$ MPa. This good property is maintained up to a thermal shock by water quench of 300 °C. The high-temperature bend strength decreases linearly with increasing temperature because of surface degradation by nitrogen above 800 °C.

The pressureless sintering ability of seven grades of the selected composition was assessed with a Doelhert matrix. A stage at 2200 °C for 2 h, allowed a density of 92.2% to be achieved for the untreated powders without additives (N10) and 97.5% with boron and carbon additives (N3). Although density is enhanced, the bend strength is not improved, probably due to a fine intergranular porosity.

References

1. Part I details?
2. R. L. PLACKETT and J. P. BURMAN, *Biometrika* **33** (1943) 305.
3. R. PHAN-TAN-LUU, D. MATHIEU and D. FENEUILLE, Fascicules de cours, L.P.R.A.I., Université d'Aix-Marseille (1983).
4. CH. BROGHAG and F. THÉVENOT, in "Ceramic Transactions, Ceramic powder Science II", edited by G. L. Messing, H. Hausner (American Ceramic Society, Westerville, Ohio, 1988) pp. 904–10.
5. F. de MESTRAL, Thesis 41 TD, Ecole Nationale Supérieure des Mines, St Etienne, France (1990).
6. W. D. KINGERY, *J. Amer. Ceram. Soc.* **38** (1955) 3.
7. G. DAS, K. S. MAZDIYASNI and H.A. LIPSITT, *ibid.* **65** (1982) 104.
8. H. PASTOR, *Ind. Céram.* **709** (1977) 573.

Received 11 June
and accepted 26 June 1990